Model-Based Predictive Control of a Concentrated Solar Plant for Heat Production

Eliott Girard, Stéphane Thil, Julien Eynard, Stéphane Grieu

PROMES–CNRS Laboratory, UPR 8521
University of Perpignan Via Domitia

24/09/25

Outline

Outline

Issue: during cloudy days, the production of concentrated solar plants is difficult to predict and can be stopped, which can hinder their ability to satisfy industrial requirements

Issue: during cloudy days, the production of concentrated solar plants is difficult to predict and can be stopped, which can hinder their ability to satisfy industrial requirements

↓

Objectives:

- Prove that solar plants equipped with parabolic trough collectors can satisfy a heat demand
- Prove that predictive control can cope with the intermittency of solar energy in various scenarios

Issue: during cloudy days, the production of concentrated solar plants is difficult to predict and can be stopped, which can hinder their ability to satisfy industrial requirements

↓

Objectives:

- Prove that solar plants equipped with parabolic trough collectors can satisfy a heat demand
- Prove that predictive control can cope with the intermittency of solar energy in various scenarios

↓

Stakes: decarbonization of industrial heat production, proof of concept

Application to a concentrated solar plant equipped with:

- 3 parabolic trough solar collectors (150 kW of maximum recoverable power)
- a thermocline tank to store energy (1100 kWh of thermal storage)
- heat exchangers to transfer thermal energy

A heat transfer fluid (HTF) flows in the plant to transport thermal energy.

Figure: MicroSol-R solar plant.

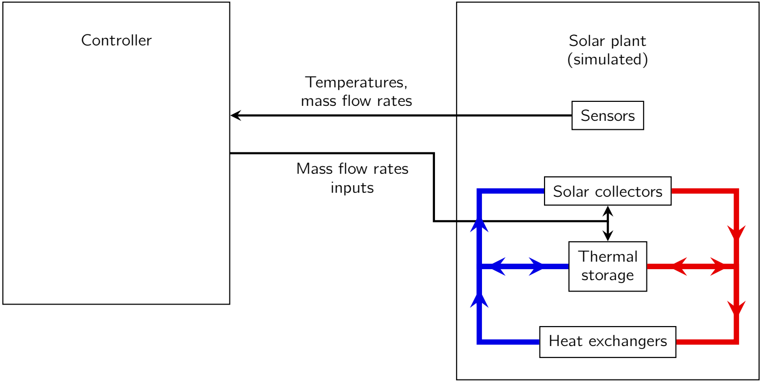

Figure: Interactions between the controller and the solar plant (the response of the plant to the mass flow inputs is simulated).

Context

Description of the controller

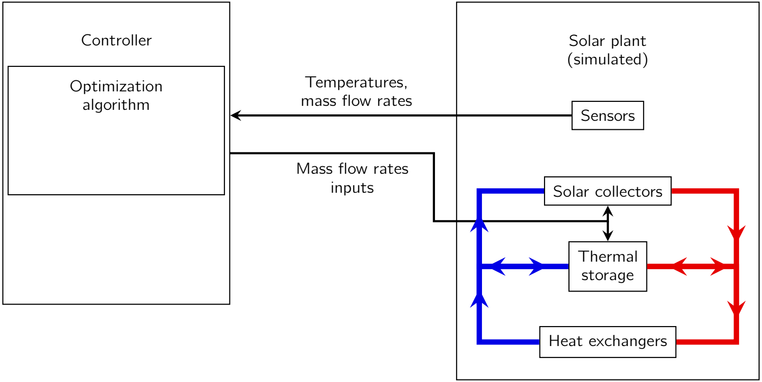

Figure: Interactions between the controller and the solar plant (the response of the plant to the mass flow inputs is simulated).

Context

Description of the controller

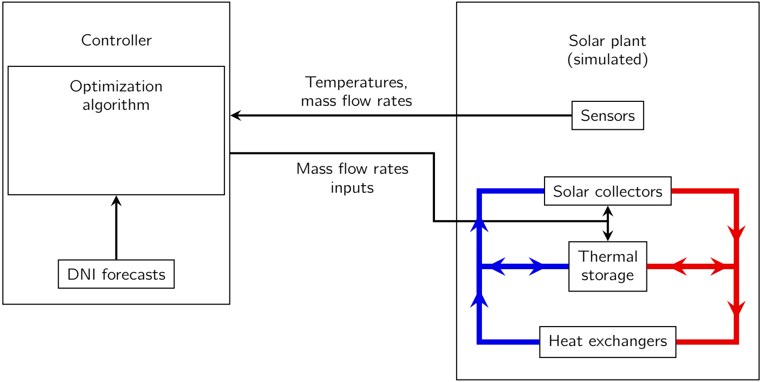

Figure: Interactions between the controller and the solar plant (the response of the plant to the mass flow inputs is simulated).

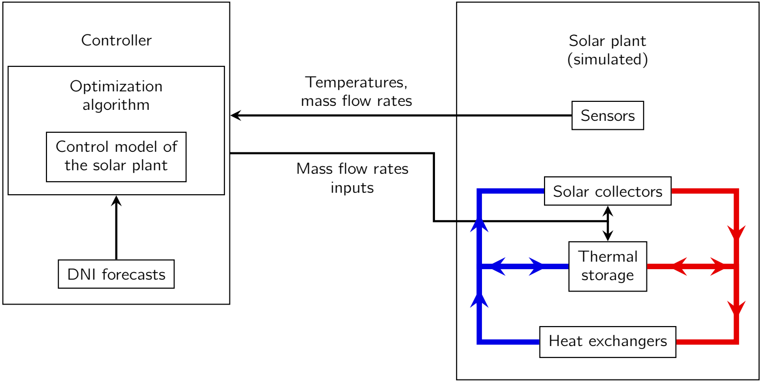

Figure: Interactions between the controller and the solar plant (the response of the plant to the mass flow inputs is simulated).

Outline

Simulation of the behaviour of a system over a given horizon to determine the control inputs to apply at the current time, and shifting the horizon each time step:

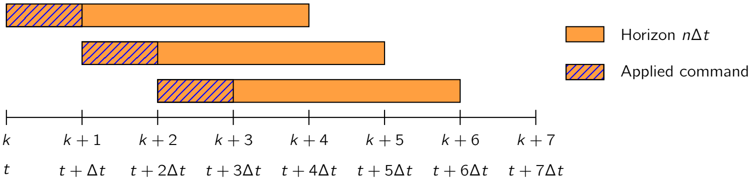

- Time step : $\Delta t = 30\,\mathrm{s}$
- Horizon : $n\Delta t = 120\,\mathrm{s}$

These parameters where evaluated to find a compromise between deviation from the heat demand and execution time.

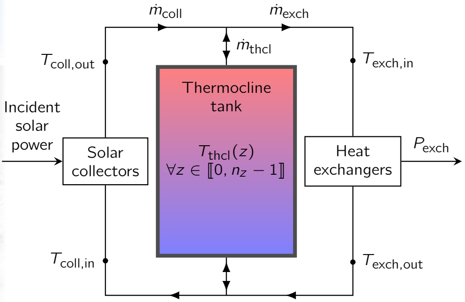

Figure: Interactions between the three systems.

Table: Variables description.

	Description
$\dot{m}_{coll}$	Mass flow inside the solar collectors
$\dot{m}_{thcl}$	Upward mass flow inside the thermocline tank
$\dot{m}_{exch}$	Mass flow inside the heat exchangers
P_{exch}	Transferred heat through the heat exchangers
DNI	Direct Normal Irradiance
T_{thcl}	HTF temperature inside the thermocline tank
$T_{coll,in}$	HTF temperature at the inlet of the solar collectors
$T_{coll,out}$	HTF temperature at the outlet of the solar collectors
$T_{exch,in}$	HTF temperature at the inlet of the heat exchangers
$T_{exch,out}$	HTF temperature at the outlet of the heat exchangers

- We want to control the exchanged thermal power P_{exch}
- We can act on the mass flows $\dot{m}_{coll}$, $\dot{m}_{thcl}$ and the incident solar power (defocus of the solar collectors)

Objective: satisfy the heat demand P_{demand} by modifying the mass flow rate inside the thermocline tank $\dot{m}_{\text{thcl}}$

$$\min_{\dot{m}_{\text{thcl}} \in \mathbb{R}^n} \quad \sqrt{\sum_{i=0}^{n-1} \left(P_{\text{exch}}(k+i) - P_{\text{demand}}(k+i)\right)^2} \tag{1}$$

$$\text{s.t.} \quad 0 < \dot{m}_{\text{thcl}}(k+i) + \dot{m}_{\text{coll}}(k+i) < \dot{m}_{\text{max}}, \ \forall i \in [\![0, n-1]\!]$$

- k: index representing the current time
- Optimization algorithm: Sequential Least Square Quadratic Programming (SLSQP)
- P_{exch}: exchanged power, calculated from a solar plant control model $\rightarrow$ the model development is the topic of an article in publication process

Algorithm 1: Control algorithm

for $k = 0$ **to** N **do**

  Initialization $\forall i \in [\![0, n-1]\!]$

    Determine $\dot{m}_{\text{coll}}(k+i)$.

    Determine $\dot{m}_{\text{thcl}}(k+i)$, to be used as optimization initialization.

end

Algorithm 1: Control algorithm

for $k = 0$ **to** N **do**

Initialization $\forall i \in [\![0, n-1]\!]$

Determine $\dot{m}_{\text{coll}}(k+i)$.

Determine $\dot{m}_{\text{thcl}}(k+i)$, to be used as optimization initialization.

Optimization $\forall i \in [\![0, n-1]\!]$

Compute the exchanged thermal power $P_{\text{exch}}(k+i)$ as a function of $\dot{m}_{\text{thcl}}(k+i)$ with a plant control model..

Outputs the optimized mass flow $\dot{m}^{*}_{\text{thcl}}(k+i)$.

end

Algorithm 1: Control algorithm

for $k = 0$ **to** N **do**

Initialization $\forall i \in [\![0, n-1]\!]$

Determine $\dot{m}_{\text{coll}}(k+i)$.

Determine $\dot{m}_{\text{thcl}}(k+i)$, to be used as optimization initialization.

Optimization $\forall i \in [\![0, n-1]\!]$

Compute the exchanged thermal power $P_{\text{exch}}(k+i)$ as a function of $\dot{m}_{\text{thcl}}(k+i)$ with a plant control model..

Outputs the optimized mass flow $\dot{m}^*_{\text{thcl}}(k+i)$.

Simulation

Simulate the plant response to the optimized $\dot{m}^*_{\text{thcl}}(k)$ using a reference plant model.

end

Outline

Performance criteria:

- deviation from the objective:

$$E_{\text{deviation}} = \sum_{k=0}^{N} |P_{\text{exch}}(k) - P_{\text{demand}}(k)|\Delta t \qquad (2)$$

- maximum overshoot:

$$\text{over}_{\max} = \max_{k} \frac{P_{\text{exch}}(k) - P_{\text{demand}}(k)}{P_{\text{demand}}(k)} \qquad (3)$$

where:

- P_{exch}: transferred power through the heat exchangers
- P_{demand}: industrial process heat demand

Simulation on 3 DNI profiles (starts at 9 a.m., ends at 5 p.m.):

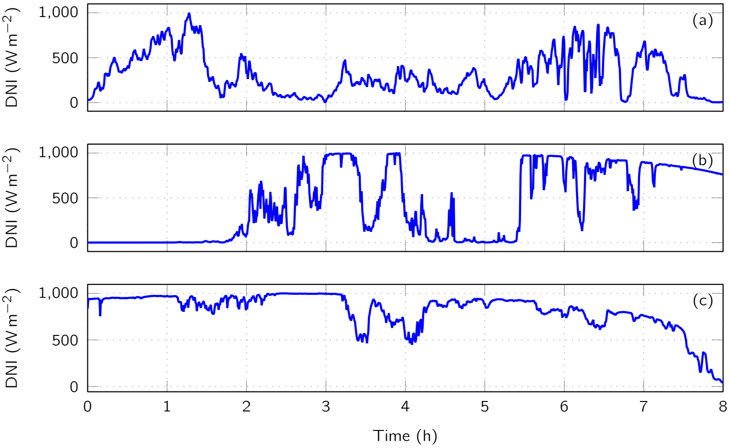

Figure: DNI profiles used as evaluation scenarios: (a) low DNI, (b) highly-varying DNI, (c) clear sky.

Control performance

Evaluation scenarios (●●○)

Simulation on 3 heat demand profiles (starts at 9 a.m., ends at 5 p.m.):

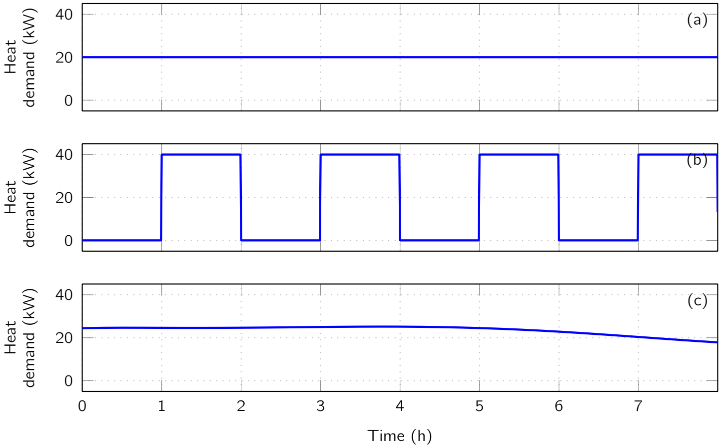

Figure: Heat demand profiles used as evaluation scenarios: (a) constant demand, (b) batch demand, (c) slowly-varying modelled industrial demand.

Control performance

Evaluation scenarios (●●●)

As industrial heat demand data is almost nonexistent, we had to use a model representing the demand of a paper industry (temperature between 100 °C and 500 °C) [1]:

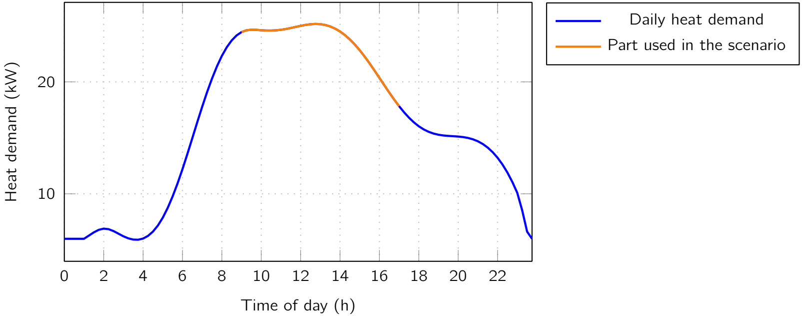

Figure: Modelled daily heat demand of a paper industry for medium temperature processes.

[1] A. Sandhaas et al. "Generation of Industrial Electricity and Heat Demand Profiles for Energy System Analysis". In: *IAEE conference proceedings* (2022).

Control performance

Influence of DNI and heat demand profiles (●○○○○○○○) — Constant demand

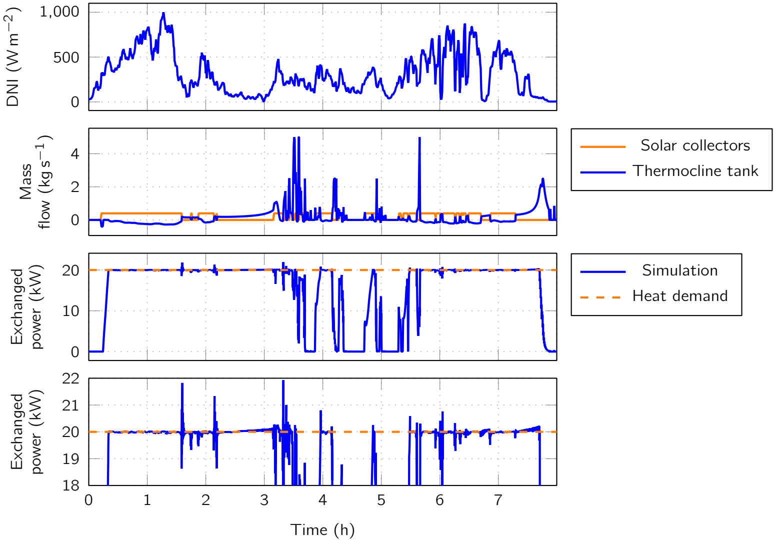

Figure: Results for the first DNI profile.

Control performance

Influence of DNI and heat demand profiles (●●○○○○○○) — Constant demand

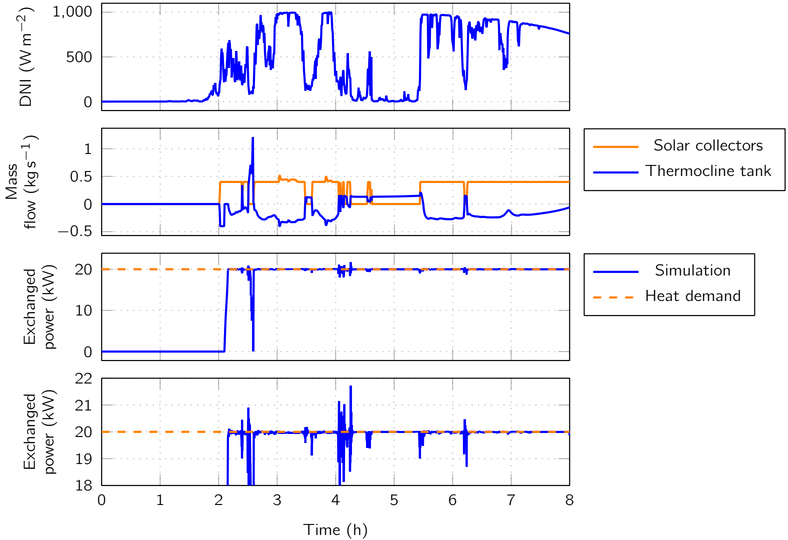

Figure: Results for the second DNI profile.

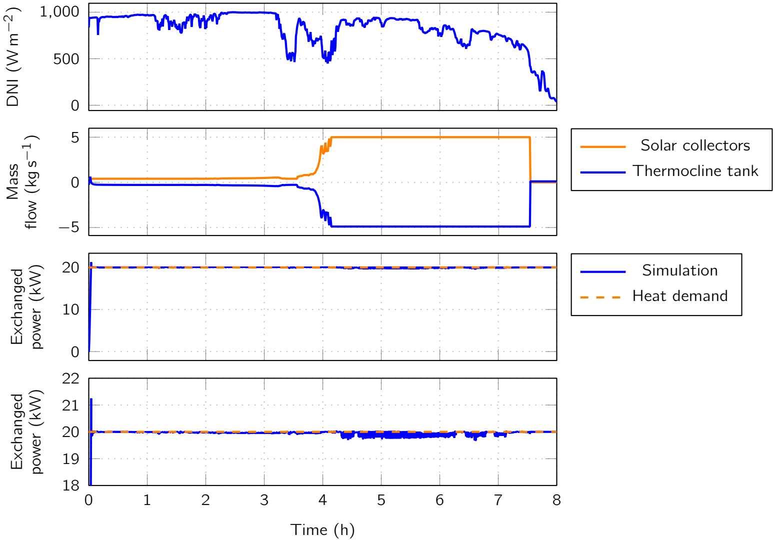

Figure: Results for the third DNI profile.

Control performance

Influence of DNI and heat demand profiles (●●●●○○○○) — Batch demand

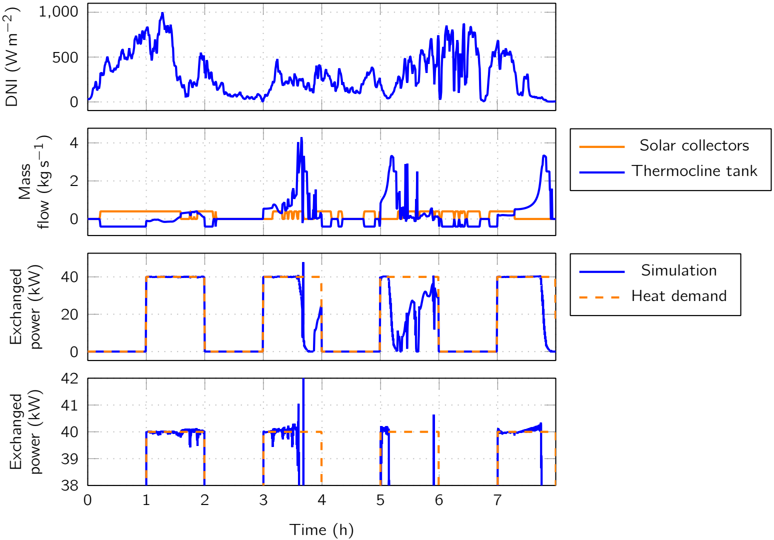

Figure: Results for the first DNI profile.

Control performance

Influence of DNI and heat demand profiles (●●●●●○○○) — Modelled industrial demand(16/21)

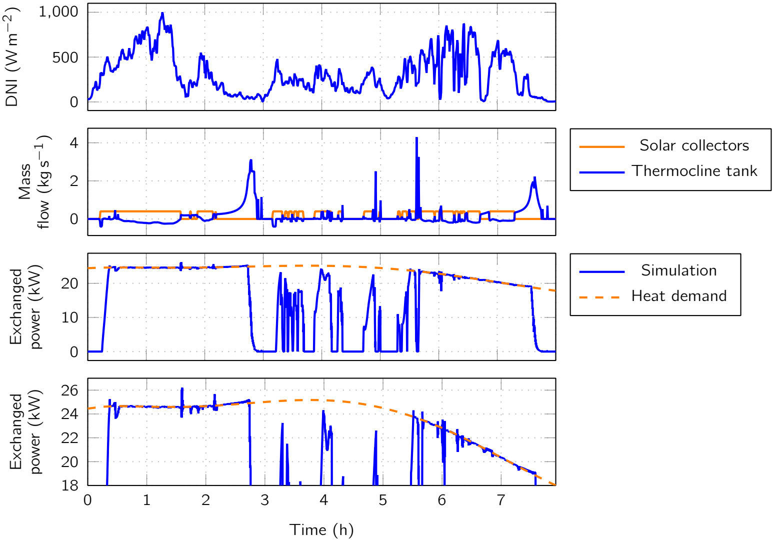

Figure: Results for the first DNI profile.

Table: Control performance in different scenarios ((a) constant demand, (b) batch demand, (c) slowly-varying modelled demand).

DNI	Low DNI			Highly-varying DNI			Clear sky		
Demand	(a)	(b)	(c)	(a)	(b)	(c)	(a)	(b)	(c)
E_{dev} (kWh)	36.95	36.92	65.40	43.32	40.29	54.86	0.79	0.39	1.00
max_{oversh} (%)	9.63	19.71	6.54	8.60	2.24	9.38	6.24	1.42	5.62

Constant demand:

- the heat demand is satisfied when possible, the high deviations are due to a lack of solar energy.
- medium overshoot (when switching from charge to discharge)

Table: Control performance in different scenarios ((a) constant demand, (b) batch demand, (c) slowly-varying modelled demand).

DNI	Low DNI			Highly-varying DNI			Clear sky		
Demand	(a)	(b)	(c)	(a)	(b)	(c)	(a)	(b)	(c)
E_{dev} (kWh)	36.95	36.92	65.40	43.32	40.29	54.86	0.79	0.39	1.00
$\max_{oversh}$ (%)	9.63	19.71	6.54	8.60	2.24	9.38	6.24	1.42	5.62

Batch demand:

- similar energy deviation to the constant demand
- low overshoot, except for low DNI

Table: Control performance in different scenarios ((a) constant demand, (b) batch demand, (c) slowly-varying modelled demand).

DNI	Low DNI			Highly-varying DNI			Clear sky		
Demand	(a)	(b)	(c)	(a)	(b)	(c)	(a)	(b)	(c)
E_{dev} (kWh)	36.95	36.92	65.40	43.32	40.29	54.86	0.79	0.39	1.00
$\max_{oversh}$ (%)	9.63	19.71	6.54	8.60	2.24	9.38	6.24	1.42	5.62

Slowly-varying modelled demand:

- higher deviation due to a slightly higher energy demand
- medium overshoot (when switching from charge to discharge)

Outline

Conclusion and perspectives

Conclusion:

- Presentation of a control strategy for concentrated solar plants equipped with parabolic trough collectors to satisfy a heat demand
- Application of this control strategy on 3 DNI profiles and 3 heat demand profiles
- The control algorithm manages to satisfy the heat demands, with little overshoot. The failure to satisfy the demand are due to a lack of solar energy.

Perspectives:

- Evaluation of the influence of DNI forecast errors
- Evaluation of control performance on a industrial-sized plant

Thank you for your attention

Questions ?

Table: Control performance in different scenarios ((a) constant demand, (b) batch demand, (c) slowly-varying modelled demand).

DNI	Low DNI			Highly-varying DNI			Clear sky		
Demand	(a)	(b)	(c)	(a)	(b)	(c)	(a)	(b)	(c)
E_{dev} (kWh)	36.95	36.92	65.40	43.32	40.29	54.86	0.79	0.39	1.00
$\max_{oversh}$ (%)	9.63	19.71	6.54	8.60	2.24	9.38	6.24	1.42	5.62

Appendix

Evaluation of the MPC time step Δt and the number of optimized variables n

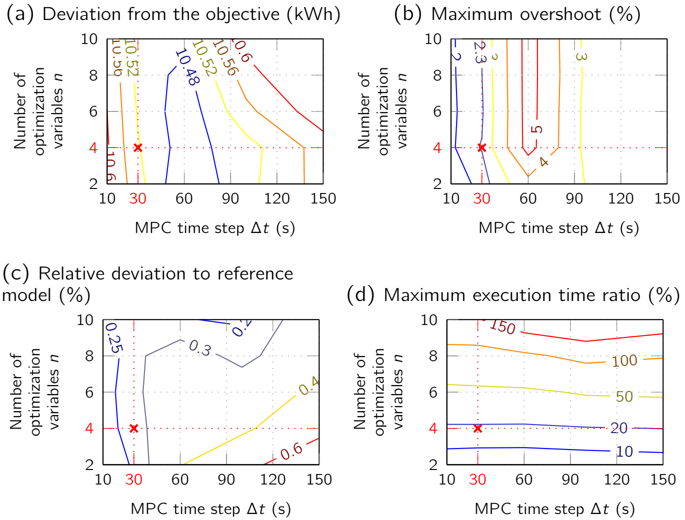

Figure: Variation of control strategy hyperparameters: Δt and n. The chosen hyperparameters are indicated by a red cross.

Computation of P_{exch} (considering a fixed outlet temperature $T_{\text{exch,out}}$):

$$P_{\text{exch}}(k) = (\dot{m}_{\text{coll}}(k) + \dot{m}_{\text{thcl}}(k)) \cdot c_{\text{f}} \cdot (T_{\text{exch,in}}(k) - T_{\text{exch,out}}(k)) \quad (4)$$

Existing model of solar collectors, fast and accurate enough to be used in the objective function [2]:

$$\begin{cases} c_{\text{f}} \dfrac{\partial T_{\text{coll}}}{\partial t} = \dot{q}_{\text{f,adv}} + \dot{q}_{\text{f,diff}} + \dot{q}_{\text{conv,f}\leftrightarrow\text{abs}} \\ c_{\text{abs}} \dfrac{\partial T_{\text{abs}}}{\partial t} = \dot{q}_{\text{abs,diff}} + \dot{q}_{\text{conv,abs}\leftrightarrow\text{f}} + \dot{q}_{\text{cond,abs}\leftrightarrow\text{ext}} + \dot{q}_{\text{ray,abs}\leftrightarrow\text{v}} + \dot{q}_{\text{abs,sol}} \\ c_{\text{v}} \dfrac{\partial T_{\text{v}}}{\partial t} = \dot{q}_{\text{v,diff}} + \dot{q}_{\text{conv,v}\leftrightarrow\text{ext}} + \dot{q}_{\text{v,sol}} + \dot{q}_{\text{ray,v}\leftrightarrow\text{abs}} + \dot{q}_{\text{ray,v}\leftrightarrow\text{ext}} \end{cases}$$

[2] T. Fasquelle et al. “A Thermal Model to Predict the Dynamic Performances of Parabolic Trough Lines”. In: *Energy* 141 (Dec. 15, 2017).

A thermocline tank model has been developped by Hoffmann [3]. This model describes the interactions between the heat transfer fluid, the solid particles and the tank's wall. It is used for the simulation step:

$$
\text{3-phase model:}\begin{cases}
c_{\mathrm{f}}\dfrac{\partial T_{\mathrm{thcl}}}{\partial t} = \dot{q}_{\mathrm{f,adv}} + \dot{q}_{\mathrm{f,diff}} + \dot{q}_{\mathrm{conv,f}\leftrightarrow\mathrm{sp}} + \dot{q}_{\mathrm{conv,f}\leftrightarrow\mathrm{w}} & \text{(6a)}\\
c_{\mathrm{sp}}\dfrac{\partial T_{\mathrm{sp}}}{\partial t} = \dot{q}_{\mathrm{sp,diff}} + \dot{q}_{\mathrm{conv,sp}\leftrightarrow\mathrm{f}} & \text{(6b)}\\
c_{\mathrm{w}}\dfrac{\partial T_{\mathrm{w}}}{\partial t} = \dot{q}_{\mathrm{w,diff}} + \dot{q}_{\mathrm{conv,w}\leftrightarrow\mathrm{f}} + \dot{q}_{\mathrm{conv,w}\leftrightarrow\mathrm{ext}} & \text{(6c)}
\end{cases}
$$

A simplified model is used in to compute the objective function:

$$
\text{Single-phase model:} \quad \left(c_{\mathrm{f}} + \frac{\rho_{\mathrm{sp}}}{\rho_{\mathrm{f}}} c_{\mathrm{sp}}\right)\frac{\partial T_{\mathrm{thcl}}}{\partial t} = \dot{q}_{\mathrm{f,adv}} \tag{7}
$$

[3] J. F. Hoffmann et al. “A Thermocline Thermal Energy Storage System with Filler Materials for Concentrated Solar Power Plants: Experimental Data and Numerical Model Sensitivity to Different Experimental Tank Scales”. In: *Applied Thermal Engineering* 100 (May 5, 2016).

Estimation of the mass flow inside the solar collectors to reach a fixed outlet temperature $T_{\mathrm{coll,out}} = 300\,^{\circ}\mathrm{C}$:

$$\rho_{\mathrm{f}} V_{\mathrm{coll}} c_{\mathrm{f}} \frac{\mathrm{d}T_{\mathrm{coll,out}}}{\mathrm{d}t} = \mathrm{DNI}(t)\eta_{\mathrm{coll}} A_{\mathrm{coll}}(1-\eta_{\mathrm{defocus}}) - \dot{m}_{\mathrm{coll}}(t) c_{\mathrm{f}} (T_{\mathrm{coll,out}}(t) - T_{\mathrm{coll,in}}(t)) \quad (8)$$

A_{coll}: solar collecting area
V_{coll}: HTF volume in the solar collectors
η_{defocus}: defocus of the solar collectors ($0 < \eta_{\mathrm{defocus}} < 1$)
η_{coll}: solar collectors efficiency